Extracellular Vesicles Induce Minimal Hepatotoxicity and Immunogenicity

Amer F. Saleh[1]*, Elisa Lázaro-Ibáñez[2]*, Malin A Forsgard[3], Olga Shatnyeva[2], Xabier Osteikoetxea[4], Fredrik Karlsson[2], Nikki Heath[4], Madeleine Ingelsten[3], Jonathan Rose[1], Jayne Harris[1], Maelle Mairesse[1], Stephanie M. Bates[1], Maryam Clausen[2], Damla Etal[2], Emilyanne Leonard[1], Mick D. Fellows[1], Niek Dekker[2], Nicholas Edmunds[1]

[1]Drug Safety and Metabolism, IMED Biotech unit, AstraZeneca, Cambridge, United Kingdom, [2]Discovery Biology, Discovery Sciences, IMED Biotech unit, AstraZeneca, Gothenburg, Sweden, [3]Drug Safety and Metabolism, IMED Biotech unit, AstraZeneca, Gothenburg, Sweden, [4]Discovery Biology, Discovery Sciences, IMED Biotech unit, AstraZeneca, Alderley Park, United Kingdom.

*Equal contribution & corresponding authors.

Amer.saleh@astrazeneca.com , tel: +441625513837

Elisa.lazaroibanez@astrazeneca.com, tel: +46725826305

Supplementary Figures

Figure S1: High-content analysis in HepG2 cells after extracellular vesicle treatment.

Figure S2: Representative histopathology images from heart, lung, and brain from PBS Control and extracellular vesicle-treated mice

Figure S3: Representative histopathology images from thymus, mesenteric lymph node, and pancreas from PBS control and extracellular vesicle-treated mice.

Figure S4: Representative histopathology images from small intestine, skeletal muscle, and tail from PBS control and extracellular vesicle-treated mice.

Supplementary Figure 1. High-content analysis in HepG2 cells after extracellular vesicle treatment. Representative images of HepG2 cells treated with PBS control (Ctrl,10% in medium), extracellular vesicles (EVs) (5 x 10^{10} particles/mL) and Chlorpromazine (CPZ, 33 µM) are shown. Cells were incubated with four different probes to assess cell death. 1 µg/mL Hoechst 33342 (blue) was used for nuclei count and nuclear size. 50 nM MitoTracker Orange (red) was used to measure the mitochondrial membrane potential. The decreased incorporation of the dye reflects a loss of mitochondrial membrane potential which can be observed in apoptotic cells with fragmented DNA (CPZ, white arrow). 1 µM TOTO-3 (green) was used to stain apoptotic and necrotic cells with compromised membrane integrity (CPZ, white arrow). Lysosomal activity was analysed using 50 nM Lysotracker Green (green). N=3 per group with six to nine image fields acquired for each using a 20 × objective.

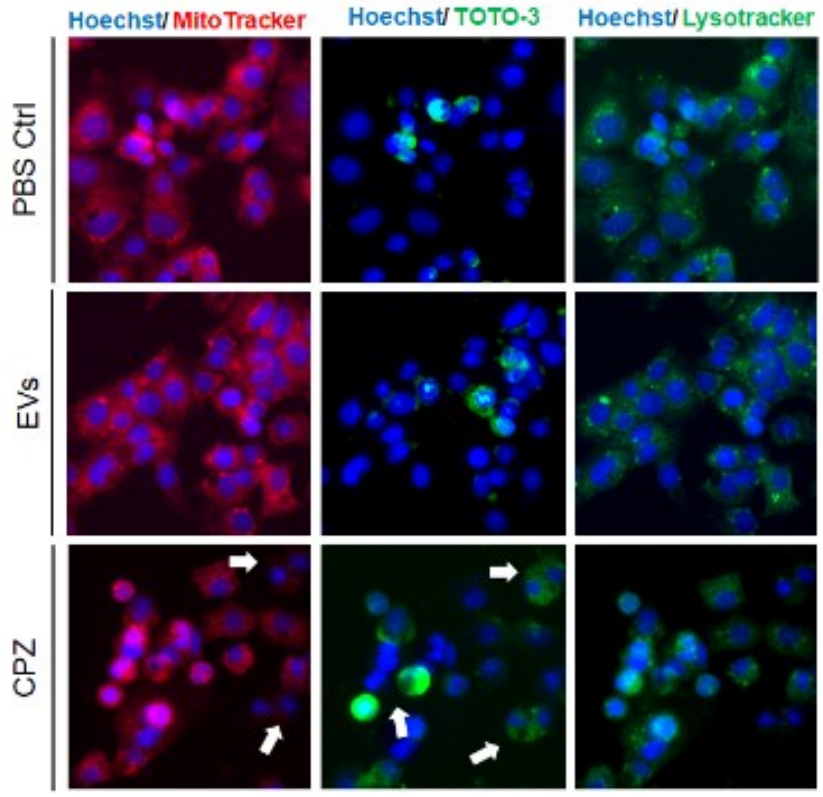

Supplementary Figure S2. Representative H&E histopathology images from heart, lung and brain from PBS control (Ctrl) and extracellular vesicle (EV)-treated mice. A, B: Longitudinal whole heart sections from (A) Ctrl and (B) EV-exposed mice. Left and right ventricular walls, ventricular septum and atria are seen. Original magnification x0.5. C, D: Lung sections from (C) Ctrl and (D) EV-exposed mice. Alveolar spaces, septal walls, terminal bronchioles, and major blood vessels are seen. Original magnification x10. E, F: Brain sections of (E) Ctrl and (F) EV-treated mice. Cerebral cortex, hippocampus and basal ganglia are seen. Original magnification x1. No noteworthy differences were observed between organs from Ctrl and EV-treated groups.

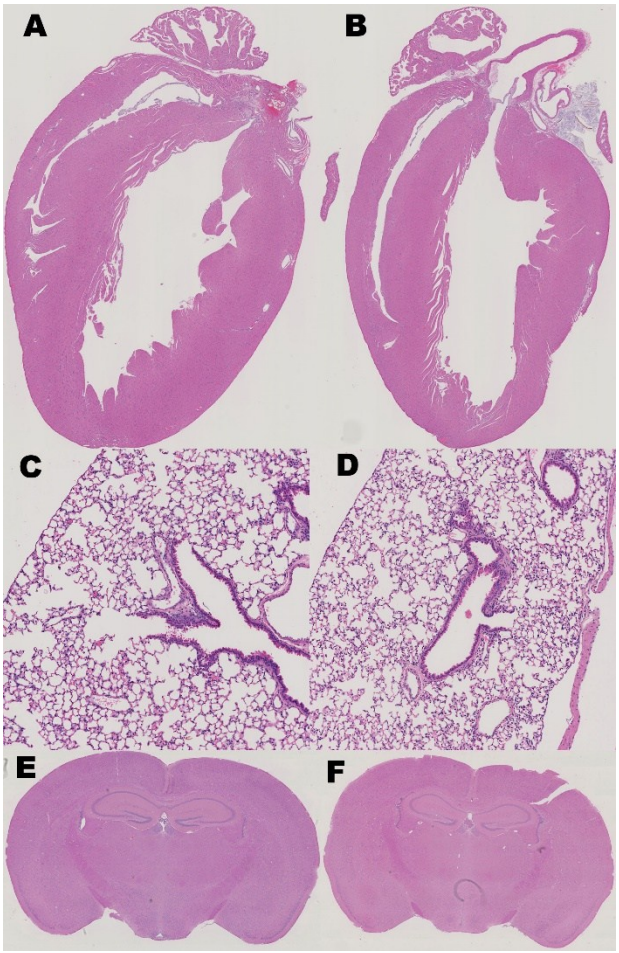

Supplementary Figure S3. Representative H&E histopathology images from thymus, mesenteric lymph node and pancreas from PBS Control (Ctrl) and extracellular vesicle (EV)-treated mice. A, B: Thymus sections from (A) Ctrl and (B) EV-treated mice. Thymus cortex and medulla are seen. Original magnification x5. C, D: Sections through mesenteric lymph node from (C) Ctrl and (D) EV-exposed mice. Germinal centres, cortex, paracortex, and lymph node sinus are seen. Magnification x10. E, F: Sections through the pancreas of (E) Ctrl and (F) EV-treated mice. Exocrine acini and endocrine islets are present. Magnification x5. No noteworthy differences were seen between organs from either group.

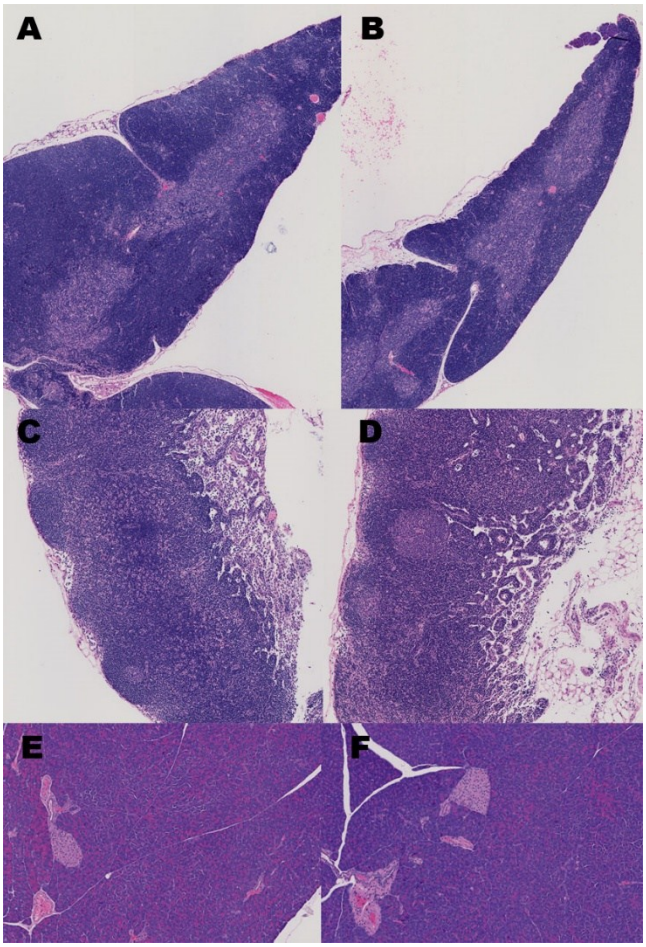

Supplementary Figure S4. Representative H&E histopathology images from small intestine, skeletal muscle and tail from PBS Control (Ctrl) and extracellular vesicle (EV)-treated mice. A, B: Transverse section from small intestine from (A) Ctrl and (B) EV-treated mice. Mucosal detail is seen with tall villi, intestinal crypts, lamina propria and muscularis. Original magnification x20. C,D: Sections through skeletal muscle from (C) Ctrl and (D) EV-treated mice. Individual muscle fibre and blood vessels are seen. Original magnification x20. E, F: Transverse sections through the tail of (E) Ctrl and (F) EV-treated mice. Lateral tail vein, adjacent structures and overlying skin are seen. Haemorrhage and inflammatory cell infiltration in the lateral tail vein and adjacent tissue is seen. Such microscopic changes are frequently seen following intravenous injections in rodents. Original magnification x20. No differences were noted between PBS-Ctrl and EV-treated animals.